Remote Influence of North Atlantic SST on the Equatorial Westerly Wind Anomalies in the Western Pacific for Initiating an El Niño Event: An Atmospheric General Circulation Model Study

Xin Wang[1, 2, 5], Chunzai Wang[2], Wen Zhou[3], Lin Liu[4], Dongxiao Wang[5]

1. *Cooperative Institute for Marine and Atmospheric Studies, University of Miami, Miami, FL, USA*
2. *NOAA/Atlantic Oceanographic and Meteorological Laboratory, Miami, FL, USA*
3. *Guy Carpenter Asia-Pacific Climate Impact Centre, School of Energy and Environment, City University of Hong Kong, Hong Kong, China*
4. *Center for Ocean and Climate Research, First Institute of Oceanography, State Oceanic Administration, Qingdao, China*
5. *State Key Laboratory of Tropical Oceanography, South China Sea Institute of Oceanology, Chinese Academy of Sciences, Guangzhou, China*

Revised to *Atmospheric Science Letters*

January 2013

Corresponding author address: Dr. Xin Wang, Physical Oceanography Division, NOAA/Atlantic Oceanographic and Meteorological Laboratory, 4301 Rickenbacker Causeway, Miami, FL 33149.
E-mail: Xin.Wang.AOML@noaa.gov

Abstract

This paper uses an AGCM to show that the cooler North Atlantic SST anomalies in summer can produce a Rossby wave-like teleconnection pattern strengthening the Siberian High in winter and next spring. The stronger Siberian High enhances the continent northerlies over East Asia and the associated cyclonic circulation over the western North Pacific, which provides a tropical westerly background for occurrence of the westerly wind bursts. The stronger northerlies over East Asia can also induce frequent cold surges, which tend to produce the equatorial westerly wind anomalies in the western Pacific for initiating an El Niño event.

Keywords: Climate, ENSO, westerly wind bursts (WWBs), El Niño Onset

1. Introduction

Many remote factors can influence on ENSO, such as the Northern Hemisphere Annular Mode (NAM, Nakamura *et al.*, 2006) and the Atlantic sea surface temperature (SST) variability (e.g. Timmermann *et al.*, 2005; Dong *et al.*, 2006; Wang, 2006; Rodríguez-Fonseca *et al.*, 2009; Wang *et al.*, 2009a; Wang *et al.*, 2009b and 2011; Ding *et al*., 2012). Nakamura *et al.* (2006) further examined the lead-lag relationship between the NAM and ENSO, and simulated the impacts of the NAM on ENSO by modulating the westerly wind bursts (WWBs). The variations in the Atlantic can influence ENSO through oceanic (Timmermann *et al.*, 2005) or atmospheric teleconnections (Dong *et al.*, 2006; Wang, 2006; Rodríguez-Fonseca *et al.,* 2009; Wang *et al.*, 2011; Ding *et al.,* 2012). Timmermann *et al.* (2005) suggested that a cooling in the North Atlantic associated with the weakened Atlantic

thermohaline circulation leads to weakened ENSO variability and results in a suppression of ENSO variance. The coupled ocean–atmosphere model results (Dong and Sutton, 2007) have suggested that the weakening ENSO variability with a deepening mean thermocline and a reduction of vertical stratification of the equatorial Pacific results from the large-scale atmospheric circulation changes associated with anomalous diabatic heating in the warm tropical Atlantic. Wang (2006) proposed that the equatorial Atlantic SST anomalies can induce an ENSO event by changing the Walker circulation and ocean dynamics, which is confirmed by modeling studies (Wang *et al.*, 2009a; Rodríguez-Fonseca *et al.*, 2009).

In addition to the impacts from the tropical Atlantic, Wang *et al.* (2009b) recently found that the ENSO variability is closely related to the North Atlantic SST variations. Moreover, Wang *et al.* (2011) proposed a possible mechanism that the North Atlantic cold SST anomalies could impact El Niño outbreak by changing the East Atlantic/West Russia teleconnection from the North Atlantic across Eurasia at the mid-latitude and the East Asian winter monsoon, which results in equatorial westerly wind anomalies and can thus initiate an El Niño event. However, these results are based on the composite and linear correlation analyses of observational data. The correlation does not necessarily guarantee a cause-effect relationship and the numerical model experiments are needed to investigate the associated physical processes linking the North Atlantic SST and westerly wind anomalies over the tropical Pacific. The purpose of the present paper is to examine the hypothesis suggested by Wang *et al.* (2011) using idealized atmospheric general circulation (AGCM) experiments. The paper demonstrates that the mechanism proposed by Wang *et al.* (2011) does operate in the AGCM simulations, thus supporting the connection between the North Atlantic cooling

and warm ENSO events.

2. Data sets and model

The data sets used in this paper include the monthly zonal wind at 10 m from the European Centre for Medium-Range Weather Forecasts (ERA40) during 1958–2001 and the monthly UK Met Office's Hadley Centre's Sea Ice and Sea Surface Temperature (HadISST1) (Rayner *et al.*, 2003). The Nino-3.4 index is calculated as SST anomalies (SSTA) averaged over the region between 5ºS–5ºN and 170ºE–120ºW. Following Wang *et al.* (2009b, 2011), a North Atlantic Index (NAI) by averaging SSTA over the region of 30º-50ºN and 10º-50ºW is used as an indicator of the North Atlantic SST variation.

The LMDZ (the Laboratoire de Météorologie Dynamique Model with Zoom Capability at Paris, France) AGCM used in this study is based on a finite-difference formulation of the primitive equations (Sadourny and Laval, 1984). The dynamical equations are discretized on a longitude-latitude Arakawa C-grid with zooming capability. Discretization in the vertical is done by using a hybrid σ–p coordinate system with 19 levels. The version of the model used in this study is described in detail by Hourdin *et al.* (2006). The current model has 120 points in longitude (evenly spaced) and 90 points in latitude, which corresponds to a resolution of 3º in longitude and 2º in latitude.

3. Results

3.1 Observed relationship between the North Atlantic and tropical Pacific

The lag correlations of the NAI index with the Nino-3.4 index and the 10 m zonal

wind in the tropical Pacific are shown in Fig. 1. It is seen that the summer North Atlantic SSTA is negatively related to the tropical eastern and central Pacific SSTA in succeeding year (note that the correlation coefficients in Fig. 1 are multiplied by -1). The significant maximum correlations are located on the eastern and central Pacific in the following winter and spring (Fig. 1a). Here, the more reliable HadISST1 during 1982-2003 is used because of in situ and bias-adjusted satellite SSTs combined from 1982 onward. These results are similar to these obtained from the longer period data (Wang *et al.*, 2011). That is to say, when there are cooler SSTA over the North Atlantic during boreal summer, the eastern and central tropical Pacific tends to be warmer in succeeding winter and spring.

An anomalous westerly wind over the tropical western Pacific is well known to trigger El Niño outbreak (Wyrtki, 1975). Therefore, we focus on the NAI-induced westerly wind anomalies over the tropical Pacific where the WWBs associated with El Niño usually occur. Figure 1b demonstrates the significant relationship between the summer North Atlantic SSTA and the zonal wind at 10 m over the central tropical Pacific prior El Niño occurrence. It is indicated that after a cooler North Atlantic in summer, the westerly wind anomalies are expected to occur over the tropical central Pacific in succeeding winter and spring, which provides a necessary condition for an El Niño outbreak (Barnett *et al.*, 1989).

3.2 Model results

We performed two groups of ensemble AGCM runs: CTRL and NATL. In the CTRL run, the AGCM is forced by climatological SST, with a model integration from January 1 to December 31 (360 days not 365 days because of the property of this model). In the NATL

run, the model is integrated from January 1 in Year (-1) to December 31 in Year (0) (720 days). Since the SST anomalies in the North Atlantic during June-July-August (JJA) are significantly correlated to the Nino-3.4 index lagging four to thirteen months, SST forcing in the NATL run is climatological value during the whole integration except for the JJA season of Year (-1). During JJA of Year (-1), the SST in the North Atlantic (30º-50ºN, 10º-50ºW) is the averaged value of different years prior to El Niño events. These selected years are 1962, 1964, 1967, 1971, 1975, 1976, 1978, 1981, 1985, 1990, 1992, 1993, and 1996, which is used in the composite analysis in Wang *et al.* (2011). These years are selected in according to the Oceanic Niño Index of NOAA from the website (http://www.cpc.ncep.noaa.gov/products/analysis_monitoring/ensostuff/ensoyears.shtml). It is noted that 6 experiments are performed based on different initial condition in both the CTRL and NATL runs. We analyze and present the ensemble mean results.

Figure 2 shows the response of anomalous wind at lower level to the cooler North Atlantic SSTA forcing from October (-1) to April (0). The significant westerly wind anomalies appear in the tropical central-eastern Pacific, which is consistent with the observed results of Wang *et al.* (2009). The wind vector with significant westerly component is seen in the region (15°S-15°N, 160°E-140°W) where the WWBs are usually identified (Harrison and Vecchi, 1997), indicating that these westerly wind anomalies could be helpful in generating eastward propagating equatorial Kelvin waves to trigger an El Niño event.

Many previous studies have shown that the westerly wind anomalies triggering El Niño are closely related to the East Asian winter monsoon (Chu, 1988; Yu and Rienecker, 1998; Zhou *et al.*, 2007a and 2007b). To explain the mechanism how the westerly wind

anomalies over the tropical Pacific respond to the North Atlantic SST variation, the large-scale atmospheric circulations over the Northern Hemisphere are analyzed. At mid-latitude from the North Atlantic across Eurasia during autumn [Oct (-1)] and spring [Apr (0)], a Rossby wave-like teleconnection at low-mid level with two anomalous positive geopotential height centers over England/Denmark and Lake Baikal and two significantly anomalous negative centers over the North Atlantic and the northeast Caspian Sea is reproduced in Fig. 3 although the positive anomalies over Lake Baikal are insignificant during Apr (0). It is known that the SST change can influence the atmosphere by altering the surface heat fluxes. The observed (Wang *et al.*, 2011) and other atmosphere-only model (Keeley *et al*., 2012) results suggest that through impacts on atmospheric heating, the cooler SST perturbations in the North Atlantic can influence not only the local atmospheric circulation but also the downstream large-scale circulation as far as in the Siberia. Our model response to a cool North Atlantic is similar to the observed result (see Fig. 8 of Wang *et al.*, 2011). It indicates that the summer cooler North Atlantic SSTA can influence the anomalous geopotential height variations over the Far East during the subsequent winter and spring, which strengthens the intensity of the Siberian High. The enhancement of the Siberian high thus results in the increasing northerly winds over the East Asia (Fig. 4). The maintenance of the stronger northerly wind anomalies indicates that there are frequent synoptic-scale cold surge events during winter and spring (Wang *et al.*, 2005), which tends to trigger WWBs and then initiate an El Niño (Chu, 1988; Yu and Rienecker, 1998). On the other hand, the stronger northwesterly wind anomalies are associated with the anomalous cyclonic circulation over the western and central North Pacific (also Fig. 2), which provide the tropical westerly

background for occurrences of the WWBs.

4. Summary

Observational data reveal a significant relationship between the North Atlantic SSTA in summer and the tropical Pacific SSTA as well as the lower-level zonal wind anomalies in the following winter and spring. El Niño is usually initiated in spring, preceded by the anomalous westerly wind over the tropical Pacific in association with cooler North Atlantic SSTA in previous summer. The AGCM experiments with summer North Atlantic SST forcing strongly confirm and support the observed results. The model experiments show how a cool North Atlantic Ocean can influence El Niño by exciting the westerly wind anomalies at low-level over the tropical central Pacific. The cool North Atlantic SST in summer can generate a Rossby wave-like teleconnection pattern at mid-latitude, which strengthens the Siberian High during winter and spring. The resultant stronger Siberian High leads to the increase of northerly winds from the mid-latitude East Asia to the tropics and induces frequent cold surge, which thus modulates WWBs over the tropical western Pacific and triggers El Niño.

It is suggested that the North Atlantic SST anomalies could influence the East Asian climate via a stationary wave-like teleconnection (Gu *et al.,* 2009; Wang *et al.*, 2011). The North Atlantic SST anomalies-induced extratropical forcing associated with El Niño is related to the East Asian winter monsoon as shown in this study. However, ENSO is suggested to link with other extratropical forcing over the North Pacific, such as the Pacific Decadal Oscillation (Chan and Zhou, 2005; Zhou *et al.*, 2007a; Wang *et al.*, 2009b) and the

North Pacific Oscillation (Alexander *et al.*, 2010). The comparison of the impacts of the North Atlantic and the North Pacific on ENSO needs to be further studied.

Acknowledgments. This work was supported by National Basic Research Program of China (2010CB950304 and 2013CB430301), National Natural Science Foundation of China (Grant Nos. 40906010 and 41175079), the Chinese Academy of Sciences, the National Oceanic and Atmospheric Administration (NOAA) Climate Program Office, and the base funding of NOAA Atlantic Oceanographic and Meteorological Laboratory (AOML).

References

Alexander MA, Vimont DJ, Chang P, Scott JD. 2010. The impact of extratropical atmospheric variability on ENSO: testing the seasonal footprinting mechanism using coupled experiments. *Journal of Climate* **23**: 2885-2901.

Barnett T, Dümenil PL, Schlese U, Roeckner E, Latif M. 1989. The effect of Eurasian snow cover on regional and global climate variations. *Journal of the Atmospheric Sciences* **46**: 661-686.

Chan JCL, Zhou W. 2005. PDO, ENSO and the summer monsoon rainfall over South China. *Geophysical Research Letters* **32**: L08810. DOI: 10.1029/2004GL022015.

Chu PS. 1988. Extratropical forcing and the burst of equatorial westerlies in the western Pacific: A synoptic study. *Journal of the Meteorological Society of Japan* **66:** 549-564.

Ding H, Keenlyside NS, Latif M. 2012. Impact of the Equatorial Atlantic on the El Niño Southern Oscillation. *Climate Dynamics* **38**: 1965-1972.

Dong BW, Sutton RT, Scaife AA. 2006. Multidecadal modulation of El Niño-Southern Oscillation (ENSO) variance by Atlantic Ocean sea surface temperatures. *Geophysical Research Letters* **33**: L08705. DOI: 10.1029/2006GL025766.

Dong BW, Sutton RT. 2007. Enhancement of ENSO variability by a weakened Atlantic thermohaline circulation in a coupled GCM. *Journal of Climate* **20**: 4920-4939.

Gu W, Li CY, Wang X, Zhou W. 2009. Linkage between mei-yu precipitation and North Atlantic SST on the decadal timescale. *Advances in Atmospheric Sciences* **26**: 101-108.

Harrison DE, Vecchi GA. 1997. Westerly wind events in the tropical Pacific, 1986-95. *Journal of Climate* **10**: 3131-3156.

Hourdin F, Musat I, Bony S, Braconnot P, Codron F, Dufresne JL, Fairhead L, Filiberti MA, Friedlingstein P, Grandpeix JY, Krinner G, Levan P, Lott F. 2006. The LMDZ4 general circulation model: climate performance and sensitivity to parametrized physics with emphasis on tropical convection. *Climate Dynamics* **27**: 787-813. DOI: 10.1007/s00382-006-0158-0.

Keeley SPE, Sutton RT, Shaffrey LC. 2012. The impact of North Atlantic sea surface temperature errors on the simulation of North Atlantic European region climate. *Quarterly Journal of the Royal Meteorological Society* **138**: 1774-1783.Nakamura T, Tachibana Y, Honda M, Yamane S. 2006. Influence of the Northern Hemisphere annular mode on ENSO by modulating westerly wind bursts. *Geophysical Research Letters* **33**: L07709. DOI: 10.1029/2005GL025432.

Rayner NA, Parker DE, Horton EB, Folland CK, Alexander LV, Rowell DP, Kent EC, Kaplan A. 2003. Global analyses of sea surface temperature, sea ice, and night marine air

temperature since the late nineteenth century. *Journal of Geophysical Research* **108**: 4407. DOI: 10.1029/2002JD002670.

Rodríguez-Fonseca B, Polo I, García-Serrano J, Losada T, Mohino E, Mechoso CR, Kucharski F. 2009. Are Atlantic Niños enhancing Pacific ENSO events in recent decades? *Geophysical Research Letters* **36**: L20705. DOI:10.1029/2009GL040048.

Sadourny R, Laval K. 1984. January and July performance of the LMD general circulation model. New Perspectives in Climate Modelling, A. Berger and C. Nicolis, Eds., Elsevier, 173-198.

Timmermann A, An SI, Krebs U, Goosse H. 2005. ENSO suppression due to weakening of the North Atlantic thermohaline circulation. *Journal of Climate* **18**: 3122-3139.

Wang C. 2006. An overlooked feature of tropical climate: Inter-Pacific-Atlantic variability. *Geophysical Research Letters* **33**, L12702, doi: 10.1029/2006GL026324.

Wang C, Kucharski F, Barimalala R, Bracco A. 2009a. Teleconnections of the tropical atlantic to the tropical Indian and Pacific Oceans: A review of recent findings. *Metorologische Zeitschrift* **18**: 445-454

Wang D, Wang C, Yang X, Lu J. 2005. Winter Northern Hemisphere surface air temperature variability associated with the Arctic Oscillation and North Atlantic Oscillation. *Geophysical Research Letters*, **32:** L16706. DOI: 10.1029/2005GL022952.

Wang X, Wang D, Zhou W. 2009b. Decadal variability of twentieth century El Niño and La Niña occurrence from observations and IPCC AR4 coupled models. *Geophysical Research Letters* **36**: L11701. DOI: 10.1029/2009GL037929.

Wang X, Wang C, Zhou W, Wang D, Song J. 2011. Teleconnected influence of North

Atlantic sea surface temperature on the El Niño onset. *Climate Dynamics* **37**: 663-676.

Wyrtki K. 1975. El Niño-the dynamic response of the equatorial Pacific Ocean to atmospheric forcing. *Journal of Physical Oceanography* **5**: 572-584.

Yu L, Rienecker MM. 1998. Evidence of an extratropical atmospheric influence during the onset of the 1997-98 El Niño. *Geophysical Research Letters* **18**: 3537-3540.

Zhou W, Li C, Wang X. 2007a. Possible connection between Pacific Oceanic interdecadal pathway and East Asian winter monsoon. *Geophysical Research Letters* **34**: L01701. DOI: 10.1029/2006GL027809.

Zhou W, Wang X, Zhou T, Li C, Chan JCL. 2007b. Interdecadal variability of the relationship between the East Asian winter monsoon and ENSO. *Meteorology and Atmospheric Physics* **98**: 283-293.

Figure Captions

Figure 1. (a) Lagged correlation coefficients between the NAI and Nino-3.4 index during 1982-2003. The X-Axis represents the months which the Nino3.4 index is lagged. The shadings indicate the correlations significant above the 90% confidence level (effective degrees of freedom are 17). (b) Linear coefficients between summer (JJA) NAI and the tropical (averaged between 10ºS and 10ºN) zonal wind at 10 m from simultaneous summer to next spring during 1958-2001. Pre El Niño of Y-Axis label means the year before El Niño onset, and El Niño indicates the onset year. The shadings indicate the correlations significant above the 90% confidence level (effective degrees of freedom are 42). In (a) and (b), the correlation coefficients are multiplied by -1. The zero contour line is thickened. The contour

interval is 0.1.

Figure 2. Evolution of the differences of wind (m s^{-1}) at 1004-hPa averaged between NATL and CTRL runs from Oct (-1) to Apr (0). The red vectors indicate the zonal wind exceeding the 90% significant level, based on Student's t test.

Figure 3. Evolution of the differences of geopotential height (m^2 s^{-2}) at 1004-hPa between NATL and CTRL runs from Oct (-1) to Apr (0). The contour interval is 0.5 m^2 s^{-2}. The zero contour line is thickened. The blue and red shadings indicate values less than -0.5 and more than 0.5, respectively. The green contours filled with the dots indicate the geopotential height exceeding the 90% significant level, based on Student's *t* test.

Figure 4. The difference of wind vector (m s^{-1}) at 847.8-hPa averaged from Dec (-1) to May (0) between NATL and CTRL runs. The red vectors indicate the meridional wind exceeding the 90% significant level, based on Student's t test.

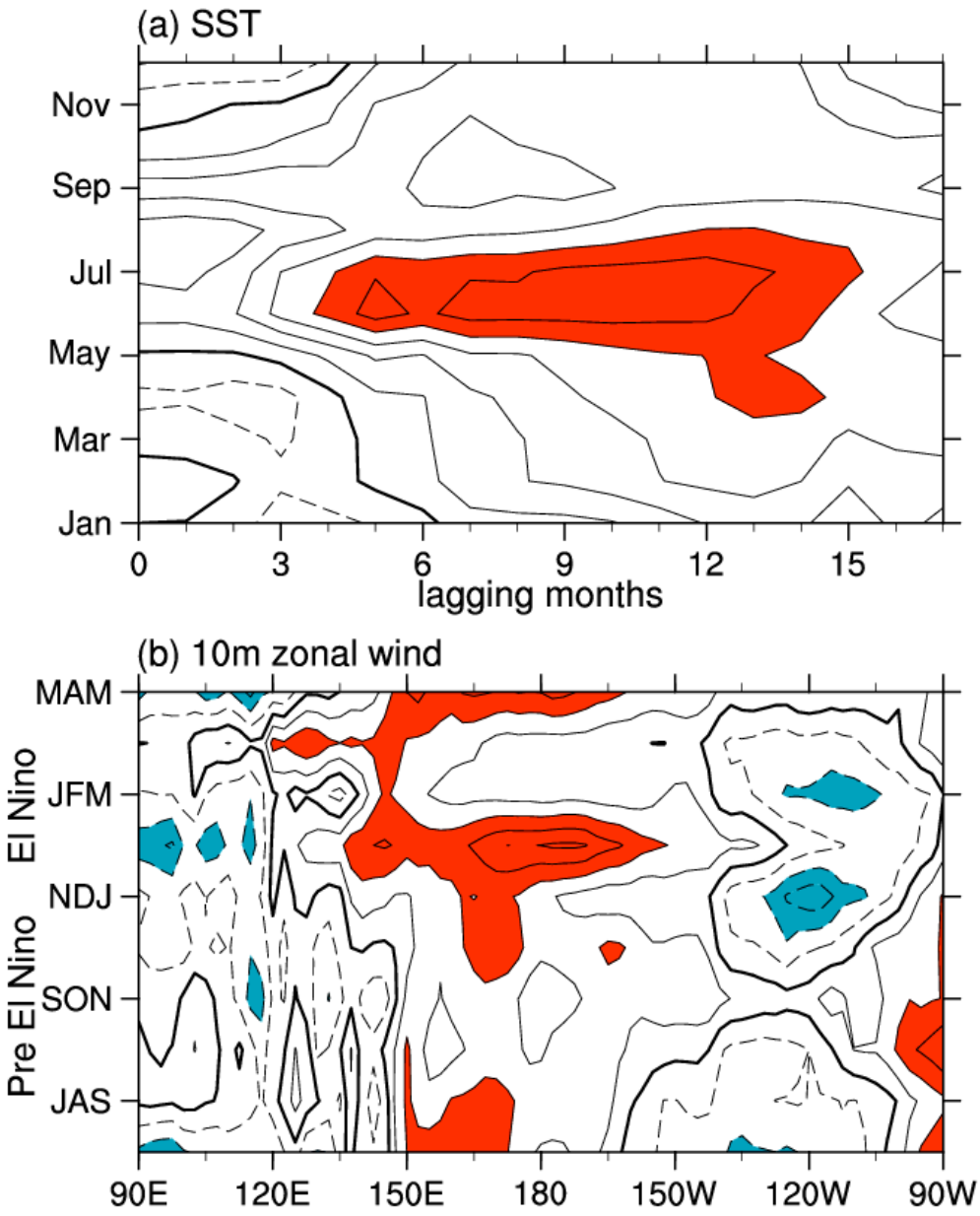

Figure 1. (a) Lagged correlation coefficients between the NAI and Nino-3.4 index during 1982-2003. The X-Axis represents the months which the Nino3.4 index is lagged. The shadings indicate the correlations significant above the 90% confidence level (effective degrees of freedom are 17). (b) Linear coefficients between summer (JJA) NAI and the tropical (averaged between 10ºS and 10ºN) zonal wind at 10 m from simultaneous summer to next spring during 1958-2001. Pre El Niño of Y-Axis label means the year before El Niño onset, and El Niño indicates the onset year. The shadings indicate the correlations significant above the 90% confidence level (effective degrees of freedom are 42). In (a) and (b), the correlation coefficients are multiplied by -1. The zero contour line is thickened. The contour interval is 0.1.

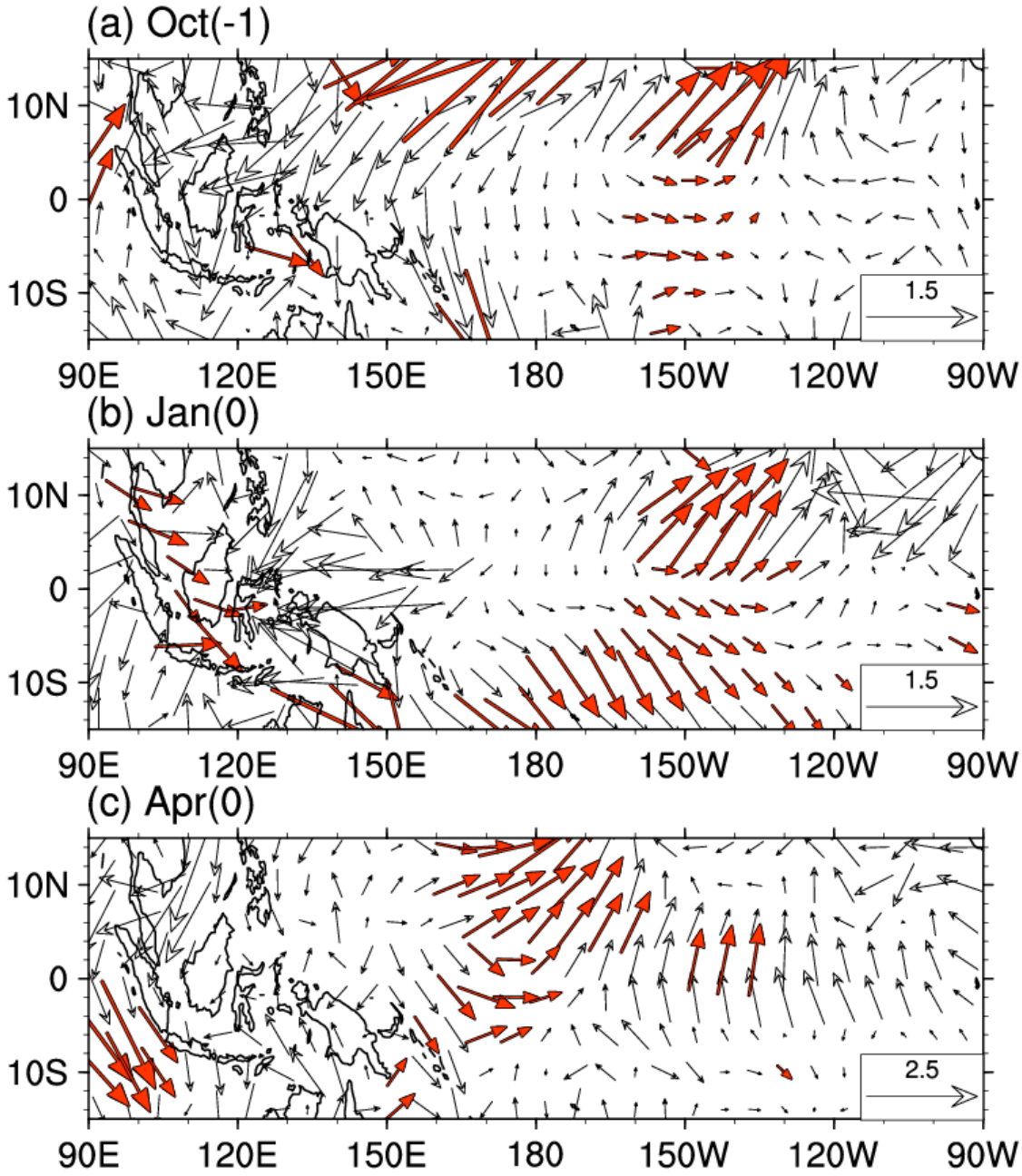

Figure 2. Evolution of the differences of wind (m s^{-1}) at 1004-hPa averaged between NATL and CTRL runs from Oct (-1) to Apr (0). The red vectors indicate the zonal wind exceeding the 90% significant level, based on Student's t test.

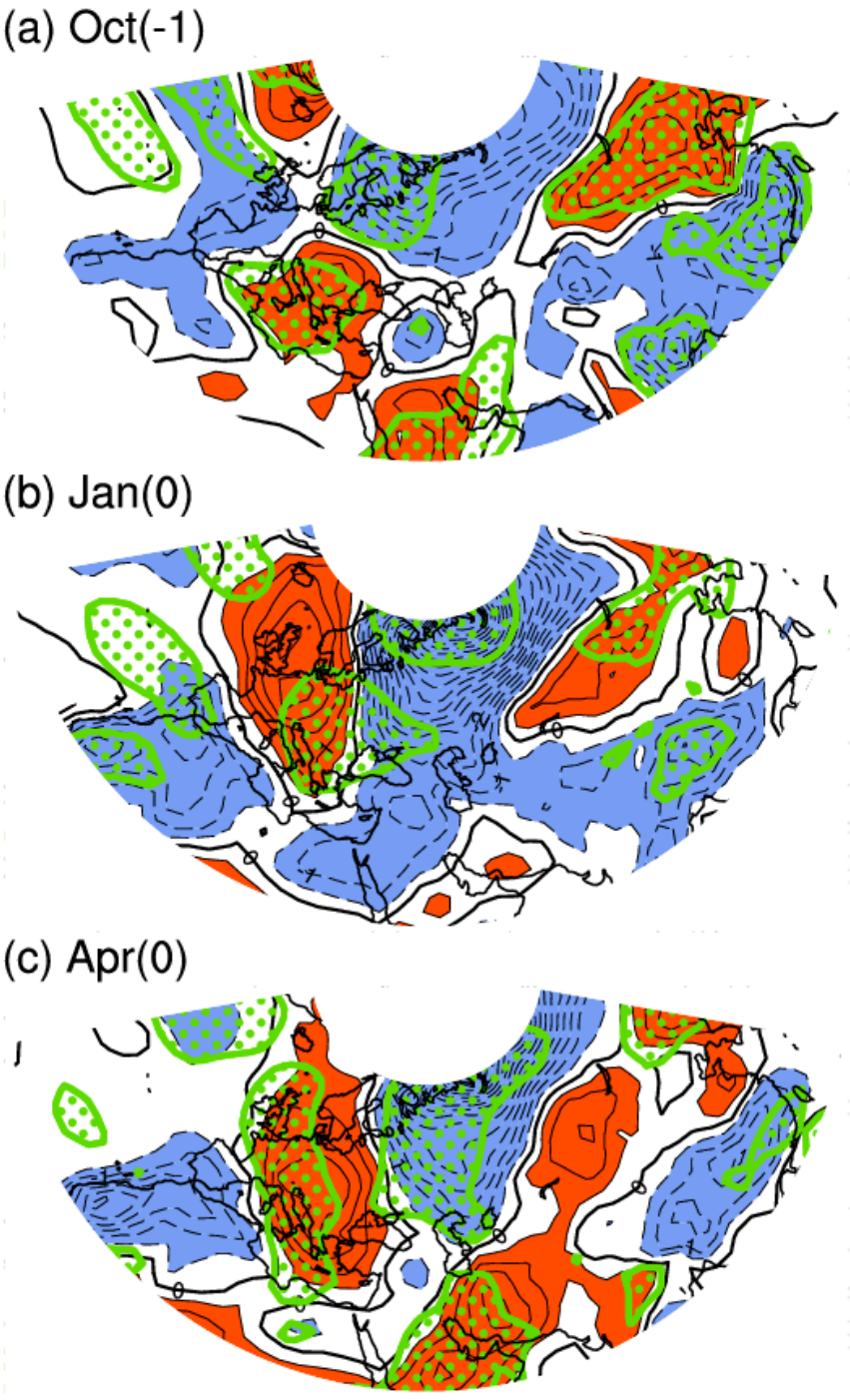

Figure 3. Evolution of the differences of geopotential height (m^2 s^{-2}) at 1004-hPa between NATL and CTRL runs from Oct (-1) to Apr (0). The contour interval is 0.5 m^2 s^{-2}. The zero contour line is thickened. The blue and red shadings indicate values less than -0.5 and more than 0.5, respectively. The green contours filled with the dots indicate the geopotential height exceeding the 90% significant level, based on Student's *t* test.

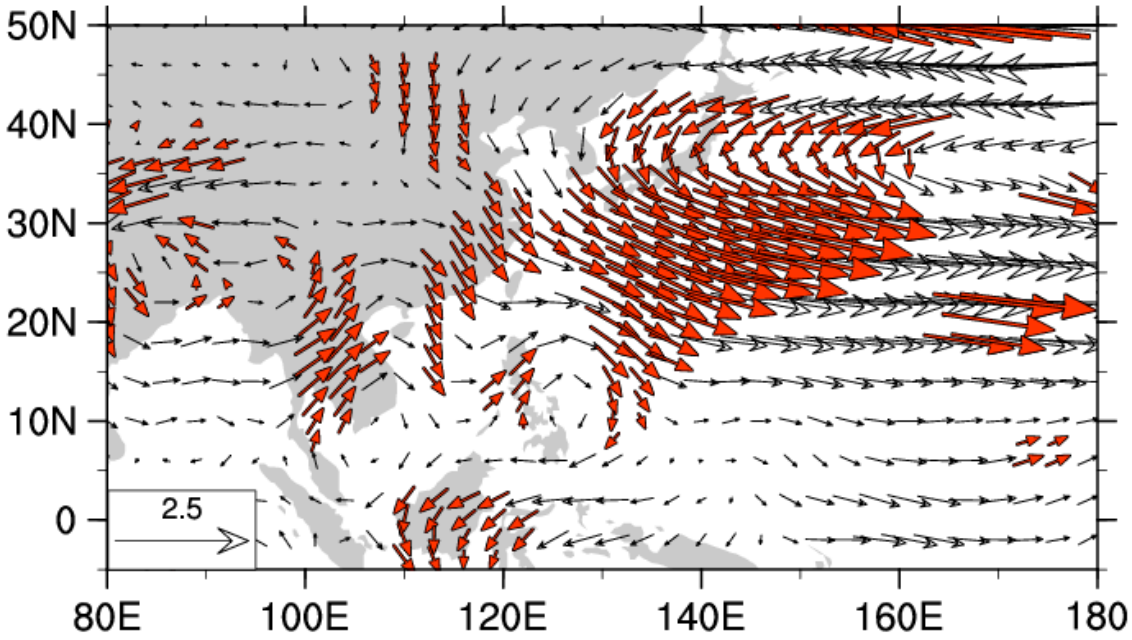

Figure 4. The difference of wind vector (m s^{-1}) at 847.8-hPa averaged from Dec (-1) to May (0) between NATL and CTRL runs. The red vectors indicate the meridional wind exceeding the 90% significant level, based on Student's t test.